Identifying the order of a quantum phase transition by means of Wehrl entropy in phase space

Octavio Castaños[*]

Instituto de Ciencias Nucleares, Universidad Nacional Autónoma de México, Apartado Postal 70-543, 04510 Distrito Federal, Mexico

Manuel Calixto[†]

Departamento de Matemática Aplicada, Facultad de Ciencias, Universidad de Granada, Fuentenueva s/n, 18071 Granada, Spain

Francisco Pérez-Bernal[‡]

Departamento de Física Aplicada, Facultad de Ciencias Experimentales, Universidad de Huelva, Campus del Carmen,
Avenida de las Fuerzas Armadas s/n, 21071 Huelva, Spain

Elvira Romera[§]

Departamento de Física Atómica, Molecular y Nuclear and Instituto Carlos I de Física Teórica y Computacional,
Universidad de Granada, Fuentenueva s/n, 18071 Granada, Spain

We propose a method to identify the order of a quantum phase transition by using area measures of the ground state in phase space. We illustrate our proposal by analyzing the well known example of the quantum cusp and four different paradigmatic boson models: Dicke, Lipkin-Meshkov-Glick, interacting boson model, and vibron model.

PACS number(s): 05.30.Rt, 05.30.Jp, 21.60.Fw, 64.70.Tg

I. INTRODUCTION

The extremely relevant concept of phase transition in thermodynamics has been extended recently to encompass novel situations. In particular, two main aspects have been recently addressed: the study of mesoscopic systems and the study of quantum systems at zero temperature. In the first case, the finite system size modifies and smooths phase transition effects. In the second case a tiny modification of a certain Hamiltonian parameter or parameters (control parameters) induces an abrupt change in the ground state of the quantum system and quantum phase transitions (QPTs) appear as an effect of quantum fluctuations at the critical value of the control parameter [1]. QPTs strictly occur in infinite systems, though QPT precursors are present in finite systems. In fact, bosonic models make it possible to study both aforementioned aspects: finite-size effects and zero temperature QPTs. Recent reviews on this subject are [2–4].

QPTs occurring in finite-size systems can be characterized by the disappearance of the gap between the ground and the first excited state energies in the mean field or thermodynamic limit (infinite system size). The QPT is a first-order phase transition if a level crossing occurs and a continuous transition if there are no crossings (except in the limit value) [5]. The Landau theory holds in the models addressed in this presentation, and within this theory the Ehrenfest classification of QPTs is valid. In this case, the order of a QPT is assigned on the basis of discontinuities in derivatives of the potential of the system at the thermodynamic limit [3,4].

The assignment of the order of a phase transitions in finite-size systems using a numerical treatment to compute finite differences of the system energy functional can be a cumbersome task. In order to overcome this problem, different approaches have been proposed. Cejnar *et al.* have used the study of non-Hermitian degeneracies near critical points to classify the order of QPTs [5]. Alternative characterizations are based in the connection between geometric Berry phases and QPTs in the case of the XY Ising model [6,7] and in the overlap between two ground state wave functions for different values of the control parameter (fidelity susceptibility concept) [8–10]. In addition, many efforts have been devoted to characterize QPTs in terms of information theoretic measures of delocalization (see [11–14] and references therein) and quantum information tools, e.g., using entanglement entropy measures (see, e.g., [15] for the Dicke model and [16,17] for the vibron model).

In this work we propose an alternative way to reckon the order of a QPT by using the Wehrl entropy in the phase-space (coherent state or Bargmann) representation of quantum states ψ provided by the Husimi function Q_ψ, which is defined as the squared overlap between ψ and an arbitrary coherent state.

The Husimi function has been widely used in quantum physics, mainly in quantum optics. For example, the time evolution of coherent states of light in a Kerr medium is visualized by measuring Q_ψ by cavity state tomography, observing quantum collapses and revivals, and confirming the nonclassical properties of the transient states [18]. Moreover, the zeros of this phase-space quasiprobability distribution have been used as an indicator of the regular or chaotic behavior in quantum maps for a variety of quantum problems: molecular [19] and atomic [20] systems, the kicked top [21], quantum billiards [22], or condensed matter systems [23] (see also [24,25] and references therein). They have also been considered as an indicator of metal insulator [26] and topological-band insulator [27] phase transitions, as well

----

[*]ocasta@nucleares.unam.mx

[†]calixto@ugr.es

[‡]francisco.perez@dfaie.uhu.es

[§]eromera@ugr.es

as of QPTs in Bose-Einstein condensates [10] and in the Dicke [28,29], vibron [17], and Lipkin-Meshkov-Glick (LMG) models [30].

To identify the order of a QPT we suggest to observe the singular behavior of the Wehrl entropy, W_ψ, of the Husimi function, Q_ψ, near the critical point as the system size increases. The Wehrl entropy is defined in Sec. III as a function of the Hamiltonian control parameter(s) and the system's size. For harmonic oscillators, Lieb proved in Ref. [31] Wehrl's conjecture [32], stating that W_ψ attains its minimum (maximum area) when ψ is an ordinary (Heisenberg-Weyl) coherent state. This proof has been recently extended by Lieb and Solovej to SU(2) spin-j systems [33]. We observe that W_ψ is maximum at the critical point of a first-order QPT, and this maximum is narrower as the system size increases. However, for second-order QPTs, the Wehrl entropy displays a step function behavior at the critical point, and again the transition is sharper for larger system sizes. We confirm this behavior for five models: quantum cusp, Dicke, LMG, a one-dimensional realization of the interacting boson model (IBM-LMG), and the two-dimensional (2D) limit of the vibron model (2DVM).

We have chosen the cusp model as a prototypical case, because this is probably the best known catastrophe example, describing the bifurcation of a critical point with a quartic potential. Its quantum version [34] has been used to illustrate the effects associated with criticality as a prior step to deal with more involved physical situations [3,34–36]. In addition to the cusp model, we present results for four different realizations of bosonic systems. The LMG model is a simple model, originally introduced for the description of nuclear systems as an exactly solvable toy model to assess the quality of different approximations [37]. This ubiquitous model still receives much attention, further stimulated by its recent experimental realization [38,39]. The study of the ground state QPTs for this model can be traced back to the seminal articles of Gilmore and Feng [40,41]. The Dicke model is a quantum-optical model that describes the interaction of a radiation field with N two-level atoms [42]. This model has recently renewed interest [43–46], partly because a tunable matter-radiation interaction is a keynote ingredient for the study of quantum critical effects [15,47,48] and partly because the model phase transition has been observed experimentally [49]. The interacting boson model (IBM) was introduced by Arima and Iachello to describe the structure of low energy states of even-even medium and heavy nuclei [50]. For the sake of simplicity, we use the IBM-LMG, a simplified version of the model built with scalar bosons [51]. Finally, the vibron model was also proposed by Iachello to describe the rovibrational structure of molecules [52] and the 2DVM was introduced [53] to model molecular bending dynamics (e.g., see Ref. [54] and references therein). The 2DVM is the simplest two-level model which still retains a nontrivial angular momentum quantum number and it has been used as a playground to illustrate ground state and excited state QPTs features in bosonic models [55,56].

We proceed to present the Hamiltonian of the five different addressed models, defining the Wehrl entropy as a function of the moments of the Husimi function Q_ψ and considering the results obtained in the first- and second-order critical points of the different models. A brief introduction to the main results

on Schwinger boson realizations, coherent states, and energy surfaces used in the paper can be found in the Appendix .

II. SELECTED MODELS

We give a brief outline of the five models we use to illustrate the characterization of QPT critical points by means of the Wehrl entropy.

The first model is the 1D quantum cusp Hamiltonian [3,34–36]

$$\hat{H} = \frac{K^2 \hat{p}^2}{2} + V_c(\hat{x}),\qquad(1)$$

where $V_c(\hat{x}) = \frac{1}{4}\hat{x}^4 + \frac{u}{2}\hat{x}^2 + v\hat{x}$ is the cusp potential, with control parameters u and v and a classicality constant $K = \frac{\hbar}{\sqrt{M}}$, combining $\hbar$ and the mass parameter M (see [35]). The smaller the value of K, the closer is the system to the classical limit. The mass parameter M can be fixed to unity without loss of generality. In order to obtain energies and eigenstates for the quantum cusp, we have recast Hamiltonian (1) in second quantization, using harmonic oscillator creation and annihilation operators and diagonalized the resulting matrix with a careful assessment of convergence. The ground state QPTs associated with the cusp have been studied using catastrophe theory and Ehrenfest's classification [3] and making use of entanglement singularities [36]. It is well known that there is a first-order QPT line when the control parameter v changes sign for negative u values and a second-order transition point for $v = 0$ and u moving from negative to positive values. In this work we consider two trajectories: (i) for $u = -1$ and $v \in [-0.2, 0.2]$ with a first-order critical point at $v_c = 0$ and (ii) for $v = 0$ and $u \in [-1, 1]$ with a second-order critical point at $u_c = 0$.

The Dicke model is an important model in quantum optics that describes a bosonic field interacting with an ensemble of N two-level atoms with level-splitting ω_0. The Hamiltonian is given by

$$\hat{H} = \omega_0 \hat{J}_z + \omega a^\dagger a + \frac{\lambda}{\sqrt{2j}}(a^\dagger + a)(\hat{J}_+ + \hat{J}_-),\qquad(2)$$

where $\hat{J}_z$, $\hat{J}_\pm$ are angular momentum operators for a pseudospin of length $j = N/2$ and a and $a^\dagger$ are the bosonic operators of a single-mode field with frequency ω. There is a second-order QPT at a critical value of the atom-field coupling strength $\lambda_c = \frac{1}{2}\sqrt{\omega\omega_0}$, with two phases: the normal phase ($\lambda < \lambda_c$) and the superradiant phase ($\lambda > \lambda_c$) [57,58]. Several tools for the identification of its QPTs have been proposed: by means of entanglement [15], information measures (see [11,13] and references therein) and in terms of fidelity [59], inverse participation ratio, the Wehrl entropy, and the zeros of the Husimi function and marginals [28,29,60].

We also deal with an interacting fermion-fermion model, the LMG model [37]. In the quasispin formalism, except for a constant term, the Hamiltonian for N interacting spins can be written as

$$\frac{\hat{H}}{2\omega j} = \frac{\hat{J}_z}{j} + \frac{\gamma_x}{j(2j-1)}\hat{J}_x^2 + \frac{\gamma_y}{j(2j-1)}\hat{J}_y^2,\qquad(3)$$

where γ_x and γ_y are control parameters. We would like to point out that the total angular momentum $J^2 = j(j+1)$ and the

number of particles $N = 2j$ are conserved and $\hat{H}$ commutes with the parity operator for fixed j. Ground-state QPTs for this model have been characterized using the continuous unitary transformation technique [61], investigating singularities in the complex plane (exceptional points) [62], and from a semiclassical perspective [63]. A complete classification of the critical points has been accomplished using the catastrophe formalism [64,65]. We study the first- and second-order QPTs given by the trajectories $\gamma_x = -\gamma_y - 4$ and $\gamma_x = -\gamma_y + 2$ in the phase diagram [65]. A characterization of QPTs in the LMG model has recently been performed in terms of Rényi-Wehrl entropies, zeros of the Husimi function, and fidelity and fidelity susceptibility concepts [30].

In the case of the characterization of the phase diagram associated with the IBM, it is important to emphasize the pioneer works on shape phase transitions on nuclei [66], which anticipated the detailed construction of the phase diagram of the IBM using either catastrophe theory [66,67], the Landau theory of phase transitions [68,69], or excited levels repulsion and crossing [70]. In the present work we use the IBM-LMG, a simplified 1D model, which shows first- and second-order QPTs, having the same energy surface as the Q-consistent IBM Hamiltonian [51]. In this case the Hamiltonian is

$$\hat{H} = x\hat{n}_t - \frac{1-x}{N}\hat{Q}^y\hat{Q}^y,$$

(4)

where $\hat{n}_t = t^\dagger t$ and $\hat{Q}^y = s^\dagger t + t^\dagger s + y\,t^\dagger t$ are expressed in terms of two species of scalar bosons s and t and the Hamiltonian has two control parameters x and y. The total number of bosons $N = \hat{n}_s + \hat{n}_t$ is a conserved quantity. For $y = 0$ there is an isolated point of second-order phase transition as a function of x with a critical value $x_c = 0.8$. For $y > 0$ the phase transition is of first order and, to illustrate this case, we have chosen the value $y = 1/\sqrt{2}$, with a critical control parameter $x_c = 0.82$.

Finally, the 2DVM is a model which describes a system containing a dipole degree of freedom constrained to planar motion. Elementary excitations are (creation and annihilation) 2D Cartesian τ bosons and a scalar σ boson. The second-order ground state QPT in this model has been studied in Ref. [56] using the essential Hamiltonian

$$\hat{H} = (1-\xi)\hat{n} + \xi\frac{N(N+1) - \hat{W}^2}{N-1},$$

(5)

where the (constant) quantum number N labels the totally symmetric representation $[N]$ of U(3), $\hat{n} = \tau_+^\dagger\tau_+ + \tau_-^\dagger\tau_-$ is the number operator of vector bosons, and $\hat{W}^2 = (\hat{D}_+\hat{D}_- + \hat{D}_-\hat{D}_+)/2 + \hat{l}^2$. The operators $\hat{D}_+ = \sqrt{2}(\tau_+^\dagger\sigma - \sigma^\dagger\tau_-)$ and $\hat{D}_- = \sqrt{2}(-\tau_-^\dagger\sigma + \sigma^\dagger\tau_+)$ are dipole operators, and $\hat{l} = \tau_+^\dagger\tau_+ - \tau_-^\dagger\tau_-$ is the angular momentum operator. This model has a single control parameter $0 \leqslant \xi \leqslant 1$ and the second-order QPT takes place at a critical value $\xi_c = 0.2$ [56]. Several procedures have been used to identify the ground state QPT in this model: entanglement entropies [16], Rényi entropies [12], the Wehrl entropy, and the inverse participation ratio of the Husimi function [71].

III. WEHRL'S ENTROPY AND GROUND STATE QPTS

We have numerically diagonalized the Hamiltonians of the five models for two different values of the system size N in an interval of control parameters containing a critical point (either first or second order). Given the expansion $|\psi\rangle = \sum_n c_n|n\rangle$ of the ground state in a basis $\{|n\rangle, n \in I\}$ (I denotes a set of quantum indices) with coefficients c_n depending on the control parameters and the system's size N and given the expansions of coherent states $|\zeta\rangle$ in the corresponding basis (see the Appendix), we can compute the Husimi function $Q_\psi(\zeta) = |\langle\zeta|\psi\rangle|^2$ and the Wehrl entropy

$$W_\psi = -\int Q_\psi(\zeta)\ln[Q_\psi(\zeta)]d\mu(\zeta),$$

(6)

where we are generically denoting by $d\mu(\zeta)$ the measure in each phase space with points labeled by ζ. Note that W_ψ is a function of the control parameters and the system size N. We discuss typical (minimum) values of W_ψ for each model, which are attained when the ground state ψ is coherent itself, and Wehrl entropy values of parity-adapted (Schrödinger cat) coherent states [72,73], which usually appear in second-order QPTs [16,17,28,30,44,45].

Cusp. In the top panels of Figs. 1 and 2 we plot W_ψ as a function of the control parameters u and v for two trajectories and two values of the classicality constant K. The first-order case is for trajectory $u = -1$, depicted in Fig. 1, with a critical control parameter $v_c = 0$. In this case a sudden growth of Wehrl entropy of the ground state at the critical point $v_c = 0$ is immediately apparent. The entropy growth is sharper as K decreases. The ground state is approximately a coherent state for $v \neq 0$ and a catlike state for $v = 0$. Indeed, as conjectured by Wehrl [32] and proved by Lieb [31], any Glauber coherent state $|\psi\rangle = |\beta\rangle$ has a minimum Wehrl entropy of $W_\psi = 1$. It has also been shown [16,28–30] that parity adapted coherent (Schrödinger cat) states, $|\psi\rangle \propto |\beta\rangle + |-\beta\rangle$, increase the minimum entropy by approximately $\ln(2)$ (for negligible overlap $\langle-\beta|\beta\rangle$). With this information, we infer that the ground state $|\psi\rangle$ is approximately a coherent state in the phase $u > 0$ and a catlike state in the phase $u < 0$.

The second-order QPT case is shown in Fig. 2, with $v = 0$ and critical control parameter $u_c = 0$. For the second trajectory, if we move from positive to negative values of u, we find in the top panel of Fig. 2 a sudden growth of W_ψ in the vicinity of the critical point $u_c = 0$ jumping from $W_\psi(u > 0) \simeq 1$ to $W_\psi(u < 0) \simeq 1 + \ln(2)$. The entropy growth is sharper as K decreases (classical limit).

Therefore, we would like to emphasize the utterly different entropic behavior of first- and second-order QPTs. In both cases we also plot an inset with the parameter trajectory and the evolution of the potential along it. We proceed to show that this Wehrl entropy behavior is shared by the rest of the considered models too, allowing a clear distinction between first- and second-order QPTs.

LMG. The LMG model has first- and second-order transitions depicted in the bottom left panels of Figs. 1 and 2, respectively. We plot W_ψ as a function of the control parameters γ_x and γ_y for the trajectories: $\gamma_y = -\gamma_x - 4$ (first-order QPT at $\gamma_{xc} = -2$, bottom left panel Fig. 1) and $\gamma_y = -\gamma_x + 2$ (second-order QPT at $\gamma_{xc} = -1$, bottom left panel Fig. 2) for
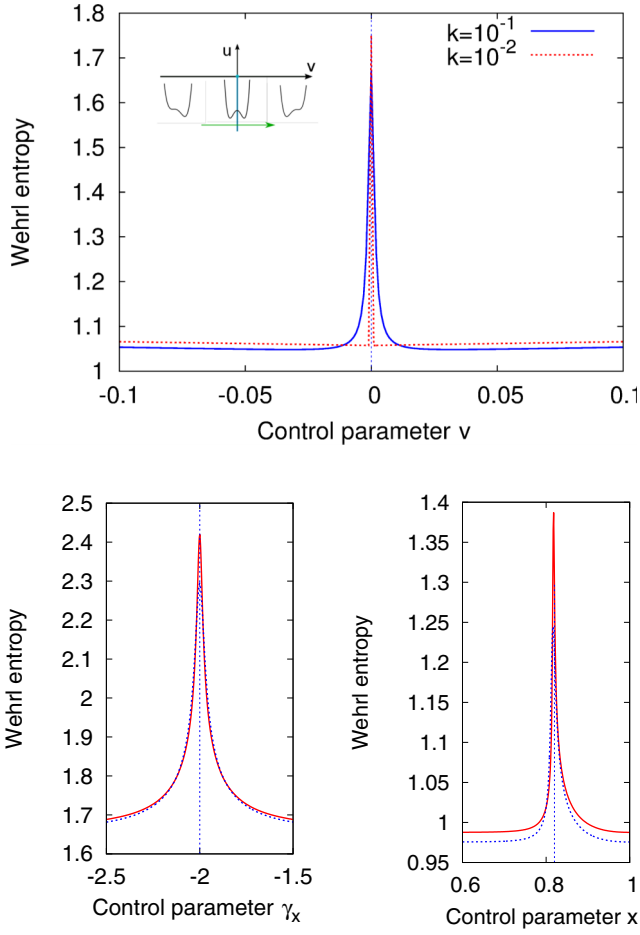
FIG. 1. (Color online) First-order QPTs: Wehrl entropy W_ψ of the Husimi function for the ground state. (Top) Cusp model for $k = 10^{-1}$ (blue solid line) and 10^{-2} (red dashed line) along the straight line $u = -1$ with critical point $v_c = 0$. (Bottom left) LMG model for $N = 20$ (blue dashed line) and 40 (red solid line) along the straight line $\gamma_x = -\gamma_y - 4$ with critical point $\gamma_{xc} = -2$. (Bottom right) IBM-LMG model for $N = 80$ (red solid line) and $N = 40$ (blue dashed line) for the straight line $y = \frac{1}{\sqrt{2}}$ with critical point $x_c = 0.82$. Critical points are marked with vertical blue dotted lines.

two values of the total number of particles N. We observe an entropic behavior completely similar to the Cusp model. The difference only lies on the particular entropy values. In fact, according to Lieb's conjecture [31,33], spin-j coherent states have a minimum Wehrl entropy of $W_\psi = \frac{2j}{2j+1}$, which tends to $W_\psi = 1$ in the thermodynamic limit $j \to \infty$. Catlike states again increase the minimum entropy by approximately $\ln(2)$. The IBM-LMG model exhibits a similar behavior to the LMG model, as can be appreciated in the bottom right panel of Figs. 1 and 2.

Dicke. The Dicke model exhibits a second-order QPT at the critical value of the control parameter $\lambda_c = 0.5$, when going from the normal ($\lambda < \lambda_c$) to the superradiant ($\lambda > \lambda_c$) phase. W_ψ captures this transition, as can be seen in the middle left panel of Fig. 2, showing an entropy increase from $W_\psi \simeq 1 + \frac{N}{N+1}$ to $W_\psi \simeq 1 + \frac{N}{N+1} + \ln(2)$, with $N = 2j$ the number of atoms. As expected, the entropic growth at λ_c is sharper for higher N.
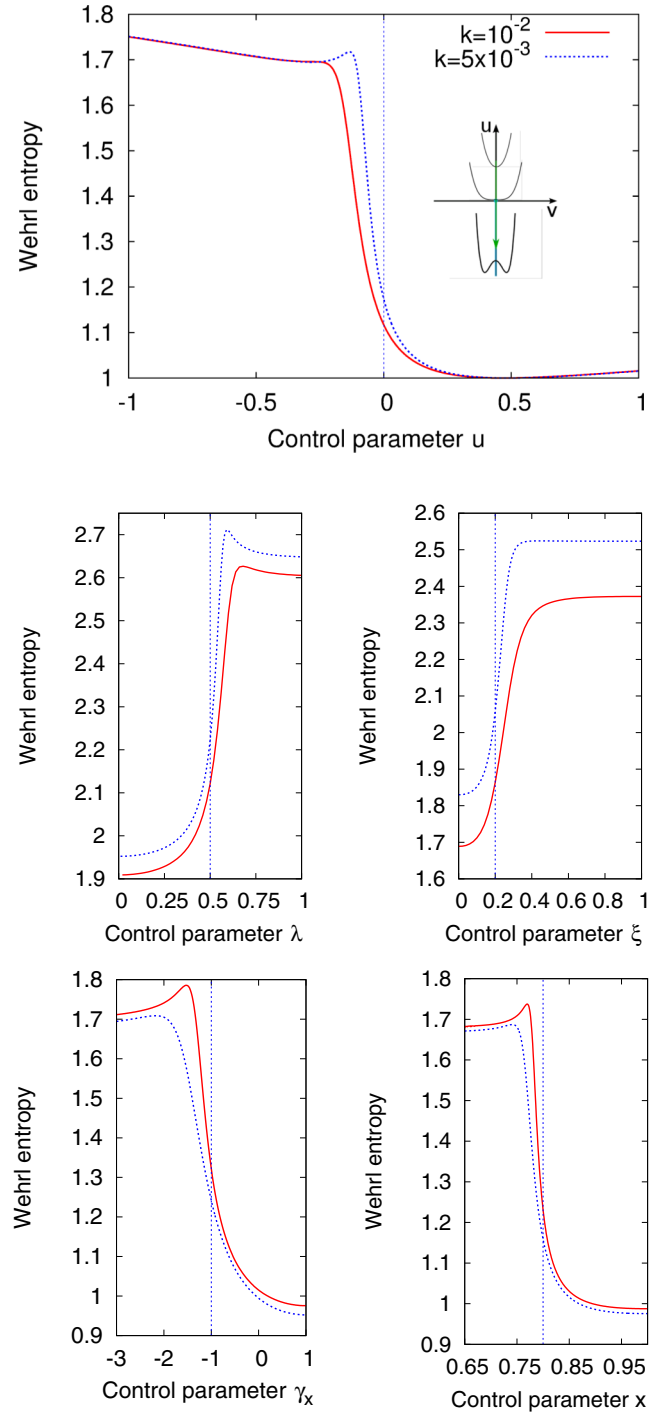

FIG. 2. (Color online) Second-order QPTs: Wehrl entropy W_ψ of the Husimi function for the ground state. (Top) Cusp model for $K = 10^{-2}$ (red solid line) and 10^{-3} (blue dashed line) along the straight line $u = 0$ with critical point $v_c = 0$. (Middle left) Dicke model for $N = 10$ (red solid line) and 20 (blue dashed line) with critical point $\lambda_c = 0.5$; (middle right) 2DVM results for $N = 8$ (red solid line) and 16 (blue dashed line) with critical point $\xi_c = 0.2$. (Bottom left) LMG model for $N = 20$ (blue dashed line) and 40 (red solid line) along the straight line $\gamma_x = -\gamma_y + 2$ with critical point $\gamma_{xc} = -1$. (Bottom right) IBM-LMG model for $N = 80$ (red solid line) and $N = 40$ (blue dashed line) for the straight line $y = 0$ with critical point $x_c = 0.8$.

Vibron. The vibron model undergoes a second-order (shape) QPT at $\xi_c = 0.2$, the critical point that marks a change between linear ($\xi < \xi_c$) and bent ($\xi > \xi_c$) phases [56]. In the middle right panel of Fig. 2 we plot the Wehrl entropy as a function of ξ for two values of the system's size N (total number of bosons). As in the previous models, the second-order QPT is characterized by a "step function" behavior of W_ψ near the critical point. In this case, we have conjectured [16] that minimum entropy $W_\psi = \frac{N(3+2N)}{(N+1)(N+2)}$ is attained for U(3) coherent states. In the bent phase, the ground state $|\psi\rangle$ is a cat [16,17,71] and therefore $W_\psi \simeq \frac{N(3+2N)}{(N+1)(N+2)} + \ln(2)$.

IV. CONCLUDING REMARKS

In summary, we have numerically diagonalized the Hamiltonians of five models for several system sizes N in a given interval of control parameters that contains a critical point (either of first or second order). Given the expansion $|\psi\rangle = \sum_n c_n |n\rangle$ of the ground state in a basis $\{|n\rangle, n \in I\}$ (where I denotes a set of quantum indices) with coefficients c_n depending on the control parameters and the system's size N, and given the expansions of coherent states in the corresponding basis, we can compute the Husimi function Q_ψ and the Wehrl entropy W_ψ. In Figs. 1 and 2 we plot W_ψ as a function of a control parameter for different values of N.

From the obtained results it is clear that the Wehrl entropy behavior at the vicinities of the critical point is an efficient numerical way of distinguishing first-order and continuous QPTs.

It is worth emphasizing that the present approach could imply an extra computational cost if compared to the search of nonanaliticities in the ground state energy functional. The present method makes use of the ground state wave functions for different values of the control parameter and it also requires the calculation of the overlap of the basis states with the coherent states. Though the need for ground state wave functions instead of ground state energies is computationally more exigent, the finer sensitivity of the present method largely offsets the extra computational cost. The second step, the overlap with coherent states, needs to be done only once with available analytic expressions (see the Appendix); therefore, it does not constitute a significant computational burden. The proposed approach permits a clear determination of the character of a critical point using relatively small basis sets. On the contrary, even for large system sizes, the numerical determination with finite differences of the critical points character could remain ambiguous.

A similar sensitivity and computational cost could be attained with the fidelity susceptibility approach, that provides a clear determination of the critical point location, but with no information of the transition order and with the additional hindrance of varying the control parameter in two different scales. Something similar happens with entanglement entropy measures, which are suitable to be applied to bipartite or multipartite systems; the critical point is clearly located, but no precise information about the transition order is obtained.

ACKNOWLEDGMENTS

APPENDIX: SCHWINGER BOSON REALIZATIONS, COHERENT STATES AND ENERGY SURFACES

a. Single mode. Radiation fields are described by harmonic oscillator creation $a^\dagger$ and annihilation a operators in Fock space $\{|n\rangle = \frac{(a^\dagger)^n}{\sqrt{n!}}|0\rangle\}$, and the corresponding normalized coherent state (CS) is given by

$$|\alpha\rangle = e^{-|\alpha|^2/2} e^{\alpha a^\dagger}|0\rangle = e^{-|\alpha|^2/2} \sum_{n=0}^{\infty} \frac{\alpha^n}{n!}|n\rangle, \quad \text{(A1)}$$

where $\alpha = x + ip \in \mathbb{C}$ is given in terms of the quadratures x, p of the field. The phase-space (Bargmann) representation of a given normalized state $|\psi\rangle = \sum_{n=0}^{\infty} c_n |n\rangle$ of the (single mode) radiation field is given by the Husimi function $Q_\psi(\alpha) = |\langle \alpha | \psi \rangle|^2$, which is normalized according to $\int_{\mathbb{R}^2} Q_\psi(\alpha) d\mu(\alpha) = 1$, with measure $d\mu(\alpha) = \frac{1}{\pi} d^2\alpha = \frac{1}{\pi} dx dp$.

b. Two-mode. (a_1, a_2) boson condensates with $N = 2j$ particles are described in terms of SU(2) operators, whose Schwinger realization is

$$J_+ = a_2^\dagger a_1, \quad J_- = a_1^\dagger a_2, \quad J_z = \tfrac{1}{2}(a_2^\dagger a_2 - a_1^\dagger a_1). \quad \text{(A2)}$$

In the case of the Dicke model, $J_\pm, J_z$ represents collective operators for an ensemble of N two-level atoms. Spin-j CSs are written in terms of the Fock basis states $|n_1 = j - m; n_2 = j + m\rangle \equiv |j,m\rangle$ (with n_1 and n_2 the occupancy number of levels 1 and 2) as

$$|\zeta\rangle = \frac{1}{\sqrt{(2j)!}} \frac{(a_2^\dagger + \zeta a_1^\dagger)^{2j}}{(1 + |\zeta|^2)^j}|0\rangle$$

$$= (1 + |\zeta|^2)^{-j} \sum_{m=-j}^{j} \binom{2j}{j+m}^{1/2} \zeta^{j+m}|j,m\rangle, \quad \text{(A3)}$$

where $\zeta = \tan(\theta/2) e^{-i\phi}$ is given in terms of the polar θ and azimuthal ϕ angles on the Riemann sphere. The phase-space representation of a normalized state $|\psi\rangle = \sum_{m=-j}^{j} c_m |j,m\rangle$ is now $Q_\psi(\zeta) = |\langle \zeta | \psi \rangle|^2$, which is normalized according to $\int_{\mathbb{S}^2} Q_\psi(\zeta) d\mu(\zeta) = 1$, with integration measure (solid angle) $d\mu(\zeta) = \frac{2j+1}{4\pi} \sin\theta d\theta d\phi$.

The IBM-LMG model, based on a scalar (s) and a pseudoscalar (t) boson creation and annihilation operators has been written in terms of SU(2) operators (A2), with $s = a_1$ and $t = a_2$.

c. Three-mode. (a_0, a_1, a_2) models (like the 2DVM) with N particles are described in terms of U(3) operators, whose Schwinger realization is $J_{jk} = a_j^\dagger a_k, j, k = 0, 1, 2$. U(3) CSs, in the symmetric representation, are written in terms of the Fock basis states $|n_0 = N - n; n_1 = (n + l)/2; n_2 = (n - l)/2\rangle \equiv |N, n, l\rangle$ [with n_j the occupancy number of level $j = 0, 1, 2$

and $n = 0, \ldots, N$ (the bending quantum number), $l = n - 2m$ (the 2D angular momentum), $m = 0, \ldots, n$] as

$$
\begin{aligned}
|\zeta_1, \zeta_2\rangle &= \frac{1}{\sqrt{N!}} \frac{(a_0^\dagger + \zeta_1 a_1^\dagger + \zeta_2 a_2^\dagger)^N}{(1 + |\zeta_1|^2 + |\zeta_2|^2)^{N/2}} |0\rangle, \\
&= \sum_{n=0}^{N} \sum_{m=0}^{n} \frac{\{N! / [(N-n)!(n-m)!m!]\}^{1/2}}{(1 + |\zeta_1|^2 + |\zeta_2|^2)^{N/2}} \\
&\quad \times \zeta_1^{n-m} \zeta_2^m |N, n, l = n - 2m\rangle, \quad \text{(A4)}
\end{aligned}
$$

with $\zeta_1, \zeta_2 \in \mathbb{C}$. The phase-space representation of a normalized state $|\psi\rangle = \sum_{n=0}^{N} \sum_{m=0}^{n} c_{nm} |N, n, l = n - 2m\rangle$ is now $Q_\psi(\zeta_1, \zeta_2) = |\langle \zeta_1, \zeta_2 | \psi \rangle|^2$, which is normalized according to $\int_{\mathbb{R}^4} Q_\psi(\zeta_1, \zeta_2) d\mu(\zeta_1, \zeta_2) = 1$, where

$$
d\mu(\zeta_1, \zeta_2) = \frac{(N+1)(N+2)}{\pi^2} \frac{d^2\zeta_1 d^2\zeta_2}{(1 + |\zeta_1|^2 + |\zeta_2|^2)^3}
$$

is the integration measure on the complex projective (quotient) space $\mathbb{C}P^2 = \mathrm{U}(3)/\mathrm{U}(2) \times \mathrm{U}(1)$ and $d^2\zeta_{1,2} \equiv d\mathrm{Re}(\zeta_{1,2})d\mathrm{Im}(\zeta_{1,2})$ the usual Lebesgue measure on $\mathbb{R}^2$.

The connection with our U(3) construction to the 2DVM is $a_0 = \sigma$ and $a_{1,2}$ are the so called circular bosons, $\tau_\pm = \mp(\tau_x \mp i\tau_y)/\sqrt{2}$, respectively.

In order to make the article as self-contained as possible, let us also briefly recall the classical Hamiltonians or energy surfaces (the Hamiltonian operator expectation value in a CS) and their critical points for the selected models. The cusp model has already been discussed in Sec. II.

For the Dicke model, using harmonic oscillator CSs (A1) for the field and spin-j CSs (A3) for the atoms, the energy surface turns out to be

$$
\langle \alpha, \zeta | \hat{H} | \alpha, \zeta \rangle = \omega |\alpha|^2 + j\omega_0 \frac{|\zeta|^2 - 1}{|\zeta|^2 + 1} + \lambda\sqrt{2j} \frac{4\mathrm{Re}(\alpha)\mathrm{Re}(\zeta)}{|\zeta|^2 + 1}. \quad \text{(A5)}
$$

Minimizing with respect to α and ζ gives the equilibrium points $\alpha_e = 0 = \zeta_e$ if $\lambda < \lambda_c$ (normal phase) and

$$
\alpha_e = -\sqrt{2j} \sqrt{\frac{\omega_0}{\omega}} \frac{\lambda}{\lambda_c} \sqrt{1 - \frac{\lambda_c^4}{\lambda^4}}, \quad \zeta_e = \sqrt{\frac{\lambda^2 - \lambda_c^2}{\lambda^2 + \lambda_c^2}}, \quad \text{(A6)}
$$

if $\lambda \geqslant \lambda_c$ (superradiant phase). For the LMG model, the energy surface written in terms of $\zeta = \tan(\theta/2)e^{-i\phi}$ is

$$
\frac{\langle \zeta | \hat{H} | \zeta \rangle}{2\omega j} = -\cos\theta + \sin^2\theta \left(\frac{\gamma_x}{2} \cos^2\phi + \frac{\gamma_y}{2} \sin^2\phi \right). \quad \text{(A7)}
$$

The minimization process results in three phases for this system: (1) region $\gamma_x < -1$ with $\gamma_x < \gamma_y$, (2) region $\gamma_y < -1$ with $\gamma_y < \gamma_x$, and (3) regions $\gamma_y > -1$ and $\gamma_x > -1$; for more information, like bifurcation sets associated with the absolute minimum of the energy surface, we address the reader to Ref. [65].

The analysis of the IBM-LMG case performed in Ref. [51] shows how for a two-mode CS $|\beta\rangle$ [the large N limit of $|\zeta\rangle$ in Eq. (A3), with $\zeta = \beta \in \mathbb{R}$] the resulting energy surface in the thermodynamic limit is

$$
\begin{aligned}
\frac{\langle \zeta | \hat{H} | \zeta \rangle}{N} &= \frac{\beta^2}{(1 + \beta^2)^2} \{5x - 4 + 4\beta y(x - 1) \\
&\quad + \beta^2 [x + y^2(x - 1)]\}, \quad \text{(A8)}
\end{aligned}
$$

which coincides with that of the Q-consistent IBM Hamiltonian [51]. If the control parameter is $y = 0$ there is an isolated second-order phase transition point as a function of the control parameter x with a critical value $x_c = 0.8$. If $y > 0$ and constant, the phase transition is of first order and minima coexistence occurs for the critical value $x_c = (4 + y^2)/(5 + y^2)$. In particular, the results shown for a first-order phase transition in the bottom right panel of Fig. 1, with $y = 1/\sqrt{2}$, are equivalent to the results obtained in the IBM model in the case of a transition from a U(5) (spherical) to a SU(3) (axially symmetric) configuration in the Casten triangle [68].

Finally, for the 2DVM [56], due to the underlying (rotational) symmetries, one can restrict himself to particular U(3) CSs (A4) with $\zeta_1 = r/\sqrt{2} = -\zeta_2$, so that the energy surface turns out to be simply

$$
\frac{\langle \zeta_1, \zeta_2 | \hat{H} | \zeta_1, \zeta_2 \rangle}{N} = (1 - \xi) \frac{r^2}{1 + r^2} + \xi \left(\frac{1 - r^2}{1 + r^2} \right)^2. \quad \text{(A9)}
$$

The minimization process results in two phase shapes: (1) linear phase ($\xi \leqslant \xi_c = 1/5$), with "equilibrium radius" $r_e = 0$, and (2) bent phase ($\xi > \xi_c$), with $r_e(\xi) = \sqrt{(5\xi - 1)/(3\xi + 1)}$.

[1] L. D. Carr, *Understanding Quantum Phase Transitions*, Series in Condensed Matter Physics (CRC Press, Taylor & Francis, Boca Raton, FL, 2010).

[2] R. F. Casten, Prog. Part. Nucl. Phys. **62**, 183 (2009).

[3] P. Cejnar and J. Jolie, Prog. Part. Nucl. Phys. **62**, 210 (2009).

[4] P. Cejnar, J. Jolie, and R. F. Casten, Rev. Mod. Phys. **82**, 2155 (2010).

[5] P. Cejnar, S. Heinze, and M. Macek, Phys. Rev. Lett. **99**, 100601 (2007).

[6] A. C. M. Carollo and J. K. Pachos, Phys. Rev. Lett. **95**, 157203 (2005).

[7] S.-L. Zhu, Phys. Rev. Lett. **96**, 077206 (2006).

[8] P. Zanardi and N. Paunković, Phys. Rev. E **74**, 031123 (2006).

[9] S.-J. Gu, Int. J. Mod. Phys. B **24**, 4371 (2010).

[10] C. Pérez-Campos, J. R. González-Alonso, O. Castaños, and R. López-Peña, Ann. Phys. **325**, 325 (2010).

[11] A. Nagy and E. Romera, Phys. A (Amsterdam, Neth.) **391**, 3650 (2012).

[12] E. Romera, R. del Real, M. Calixto, S. Nagy, and A. Nagy, J. Math. Chem. **51**, 620 (2013).

[13] E. Romera, M. Calixto, and A. Nagy, Europhys. Lett. **97**, 20011 (2012).

[14] A. Nagy and E. Romera, Europhys. Lett. **109**, 60002 (2015).

[15] N. Lambert, C. Emary, and T. Brandes, Phys. Rev. A **71**, 053804 (2005).

[16] M. Calixto, E. Romera, and R. del Real, J. Phys. A **45**, 365301 (2012).

[17] M. Calixto and F. Pérez-Bernal, Phys. Rev. A **89**, 032126 (2014).

[18] G. Kirchmair *et al.*, Nature (London) **495**, 205 (2013).

[19] F. J. Arranz, Z. S. Safi, R. M. Benito, and F. Borondo, Eur. Phys. J. D **60**, 279 (2010).

[20] P. A. Dando and S. Monteiro, J. Phys. B **27**, 2681 (1994).

[21] S. Chaudhury *et al.*, Nature (London) **461**, 768 (2009).

[22] J.-M. Tualle and A. Voros, Chaos, Solitons Fractals **5**, 1085 (1995).

[23] D. Weinmann, S. Kohler, G.-L. Ingold, and P. Hänggi, Ann. Phys. (Leipzig) **8**, SI277 (1999).

[24] P. Leboeuf and A. Voros, J. Phys. A **23**, 1765 (1990).

[25] F. J. Arranz, L. Seidel, C. G. Giralda, R. M. Benito, and F. Borondo, Phys. Rev. E **87**, 062901 (2013).

[26] C. Aulbach *et al.*, New J. Phys. **6**, 70 (2004).

[27] M. Calixto and E. Romera, Europhys. Lett. **109**, 40003 (2015).

[28] R. del Real, M. Calixto, and E. Romera, Phys. Scr., T**153**, 014016 (2013).

[29] E. Romera, R. del Real, and M. Calixto, Phys. Rev. A **85**, 053831 (2012).

[30] E. Romera, M. Calixto, and O. Castaños, Phys. Scr. **89**, 095103 (2014).

[31] E. H. Lieb, Commun. Math. Phys. **62**, 35 (1978).

[32] A. Wehrl, Rep. Math. Phys. **16**, 353 (1979).

[33] E. H. Lieb and J. P. Solovej, Acta Math. **212**, 379 (2014).

[34] R. Gilmore, S. Kais, and R. D. Levine, Phys. Rev. A **34**, 2442 (1986).

[35] P. Cejnar and P. Stránský, Phys. Rev. E **78**, 031130 (2008).

[36] C. Emary, N. Lambert, and T. Brandes, Phys. Rev. A **71**, 062302 (2005).

[37] H. Lipkin, N. Meshkov, and A. Glick, Nucl. Phys. **62**, 188 (1965).

[38] P. Jurcevic *et al.*, Nature (London) **511**, 202 (2014).

[39] P. Richerme *et al.*, Nature (London) **511**, 198 (2014).

[40] R. Gilmore and D. H. Feng, Nucl. Phys. A **301**, 189 (1978).

[41] R. Gilmore and D. H. Feng, Phys. Lett. B **76**, 26 (1978).

[42] R. H. Dicke, Phys. Rev. **93**, 99 (1954).

[43] B. M. Garraway, Philos. Trans. R. Soc. A **369**, 1137 (2011).

[44] O. Castaños, E. Nahmad-Achar, R. López-Peña, and J. G. Hirsch, Phys. Rev. A **83**, 051601 (2011).

[45] O. Castaños, E. Nahmad-Achar, R. López-Peña, and J. G. Hirsch, Phys. Rev. A **84**, 013819 (2011).

[46] P. Nataf and C. Ciuti, Nat. Commun. **1**, 72 (2010).

[47] C. Emary and T. Brandes, Phys. Rev. Lett. **90**, 044101 (2003).

[48] C. Emary and T. Brandes, Phys. Rev. E **67**, 066203 (2003).

[49] K. Baumann, C. Guerlin, F. Brennecke, and T. Esslinger, Nature (London) **464**, 1301 (2010).

[50] F. Iachello and A. Arima, *The Interacting Boson Model* (Cambridge University Press, Cambridge, UK, 1987).

[51] J. Vidal, J. M. Arias, J. Dukelsky, and J. E. García-Ramos, Phys. Rev. C **73**, 054305 (2006).

[52] F. Iachello, Chem. Phys. Lett. **78**, 581 (1981).

[53] F. Iachello and S. Oss, J. Chem. Phys. **104**, 6956 (1996).

[54] D. Larese, F. Pérez-Bernal, and F. Iachello, J. Mol. Struct. **1051**, 310 (2013).

[55] M. Caprio, P. Cejnar, and F. Iachello, Ann. Phys. **323**, 1106 (2008).

[56] F. Pérez-Bernal and F. Iachello, Phys. Rev. A **77**, 032115 (2008).

[57] K. Hepp and E. H. Lieb, Ann. Phys. **76**, 360 (1973).

[58] Y. K. Wang and F. T. Hioe, Phys. Rev. A **7**, 831 (1973).

[59] O. Castaños, E. Nahmad-Achar, R. López-Peña, and J. G. Hirsch, Phys. Rev. A **86**, 023814 (2012).

[60] M. A. Bastarrachea-Magnani *et al.*, arXiv:1509.05918.

[61] S. Dusuel and J. Vidal, Phys. Rev. Lett. **93**, 237204 (2004).

[62] W. D. Heiss, F. G. Scholtz, and H. B. Geyer, J. Phys. A: Math. Gen. **38**, 1843 (2005).

[63] F. Leyvraz and W. D. Heiss, Phys. Rev. Lett. **95**, 050402 (2005).

[64] O. Castaños, R. López-Peña, J. G. Hirsch, and E. López-Moreno, Phys. Rev. B **72**, 012406 (2005).

[65] O. Castaños, R. López-Peña, J. G. Hirsch, and E. López-Moreno, Phys. Rev. B **74**, 104118 (2006).

[66] D. H. Feng, R. Gilmore, and S. R. Deans, Phys. Rev. C **23**, 1254 (1981).

[67] E. López-Moreno and O. Castaños, Phys. Rev. C **54**, 2374 (1996).

[68] F. Iachello, N. V. Zamfir, and R. F. Casten, Phys. Rev. Lett. **81**, 1191 (1998).

[69] J. Jolie, P. Cejnar, R. F. Casten, S. Heinze, A. Linnemann, and V. Werner, Phys. Rev. Lett. **89**, 182502 (2002).

[70] J. M. Arias, J. Dukelsky, and J. E. García-Ramos, Phys. Rev. Lett. **91**, 162502 (2003).

[71] M. Calixto, R. del Real, and E. Romera, Phys. Rev. A **86**, 032508 (2012).

[72] O. Castaños, R. Lopez-Peña, and V. Manko, J. Russ. Laser Res. **16**, 477 (1995).

[73] O. Castaños and J. A. López-Saldívar, J. Phys.: Conf. Ser. **380**, 012017 (2012).